Truncated RAP-MUSIC (TRAP-MUSIC) for MEG and EEG source localization

Mäkelä , Niko

2018-02-15

Mäkelä , N , Stenroos , M , Sarvas , J & Ilmoniemi , R J 2018 , ' Truncated RAP-MUSIC
þÿ (T R A P - M U S I C) f o r M E G a n d E E G s o u r c e l o c a l i z a t i o n ' , N e u r o I m a g e , v

http://hdl.handle.net/10138/300720
https://doi.org/10.1016/j.neuroimage.2017.11.013

publishedVersion

NeuroImage 167 (2018) 73–83

Contents lists available at ScienceDirect

NeuroImage

journal homepage: www.elsevier.com/locate/neuroimage

Truncated RAP-MUSIC (TRAP-MUSIC) for MEG and EEG source localization

Niko Mäkelä [a,b,*], Matti Stenroos [a], Jukka Sarvas [a], Risto J. Ilmoniemi [a,b]

[a] Department of Neuroscience and Biomedical Engineering (NBE), Aalto University School of Science, Espoo, Finland
[b] BioMag Laboratory, HUS Medical Imaging Center, Helsinki University Hospital (HUH), Helsinki, Finland

ARTICLE INFO

Keywords:
Magnetoencephalography
Electroencephalography
MEG
EEG
Source localization
Inverse methods
Multiple sources

ABSTRACT

Electrically active brain regions can be located applying MUltiple SIgnal Classification (MUSIC) on magneto- or electroencephalographic (MEG; EEG) data. We introduce a new MUSIC method, called truncated recursively-applied-and-projected MUSIC (TRAP-MUSIC). It corrects a hidden deficiency of the conventional RAP-MUSIC algorithm, which prevents estimation of the true number of brain-signal sources accurately. The correction is done by applying a sequential dimension reduction to the signal-subspace projection. We show that TRAP-MUSIC significantly improves the performance of MUSIC-type localization; in particular, it successfully and robustly locates active brain regions and estimates their number. We compare TRAP-MUSIC and RAP-MUSIC in simulations with varying key parameters, *e.g.*, signal-to-noise ratio, correlation between source time-courses, and initial estimate for the dimension of the signal space. In addition, we validate TRAP-MUSIC with measured MEG data. We suggest that with the proposed TRAP-MUSIC method, MUSIC-type localization could become more reliable and suitable for various online and offline MEG and EEG applications.

Introduction

Multiple signal classification (MUSIC) and its recursively-applied version (RAP-MUSIC) are standard methods for locating active brain regions in magneto- and electroencephalography (MEG/EEG). MUSIC-type source localization is based on dividing the data space into signal and noise subspaces, and testing for each candidate source in the region-of-interest (ROI), whether its topography belongs to the signal subspace or not Schmidt (1986); Mosher and Leahy (1999).

Thanks to their simplicity/intuitiveness, computational efficiency, and insensitivity to measurement noise as well as to temporal correlations between the active sources, MUSIC methods, especially RAP-MUSIC, have been found useful in various offline and online MEG/EEG applications (Mosher and Leahy, 1999; Mosher et al., 1999; Dinh et al., 2012, 2014). MUSIC-framework offers probably one of the simplest inverse methods that incorporates both spatial and temporal information in source localization from EEG/MEG (Mosher and Leahy, 1999). MUSIC is closely related to beamformers, which are extensively used in analysis of EEG/MEG (Sekihara and Nagarajan, 2008). One difference is that, unlike beamformers, MUSIC does not provide the time-courses during the localization process; they need to be estimated separately. Unlike beamformer, the MUSIC procedure does not require the inversion of the data covariance matrix. MUSIC should also tolerate time-correlated sources better, as uncorrelatedness is not assumed in defining the MUSIC localizer. Furthermore, RAP-MUSIC provides an important solution to the difficult peak-detection problem of the basic MUSIC, and allows a straightforward automation of the multiple source localization task (Mosher and Leahy, 1999). While RAP-MUSIC can be used in analyzing EEG/MEG offline for both event-related (Pascarella et al., 2010; Cheyne et al., 2006) and spontaneous brain signals (Ewald et al., 2014; Baker et al., 2014; Groβ et al., 2001), it's computational efficiency makes it a particularly intriguing tool for online applications, such as closed-loop EEG systems and brain–computer interfaces (Dinh et al., 2012, 2014; Sanchez et al., 2014; Birbaumer et al., 2009).

However, we tested the performance of RAP-MUSIC on simulated EEG data and observed that it systematically overestimated the number of the sources, *i.e.*, it gave false positives. This raised a question whether there is something wrong or suboptimal in the conceptually beautiful RAP-MUSIC. Therefore, we decided to investigate the RAP-MUSIC algorithm in detail.

We introduce a novel recursive MUSIC-type method called truncated RAP-MUSIC (TRAP-MUSIC), which corrects a hidden limitation in the conventional RAP-MUSIC algorithm. We call this limitation 'the RAP dilemma'. Due to the RAP dilemma, the recursive process may leave unwanted residuals to the data model; these residuals can lead to high localizer values and thus to misleading interpretation of the location and

* Corresponding author. Department of Neuroscience and Biomedical Engineering (NBE), Aalto University School of Science, Espoo, Finland.
E-mail address: niko.makela@aalto.fi (N. Mäkelä).

https://doi.org/10.1016/j.neuroimage.2017.11.013
Received 6 June 2017; Received in revised form 18 October 2017; Accepted 4 November 2017
Available online 8 November 2017

number of the sources. We explain and analyze the RAP dilemma both theoretically and in numerical simulations, and show how TRAP-MUSIC overcomes this problem. TRAP-MUSIC is a 'corrected' version of the conventional RAP-MUSIC; TRAP-MUSIC applies a sequential dimension reduction to the signal-space estimate. We show that our correction allows robust and reliable estimation of the number of the sources, which is often not possible with RAP-MUSIC.

New MUSIC methods have been recently developed to serve in specific applications, *e.g.*, for locating extended sources (ExSo-MUSIC (Birot et al., 2011);), or for locating synchronous activity, either by exploiting source clustering (POP-MUSIC (Liu and Schimpf, 2006);), or the imaginary part of the cross-spectrum (Wedge-MUSIC; (Ewald et al., 2014), SC-MUSIC (Shahbazi et al., 2015);). We point out that most of these MUSIC variations have added their modifications *on top* of the conventional RAP-MUSIC; they first apply RAP-MUSIC, and subsequently apply their novel extra step. Therefore, it is possible that at least some issues due to the RAP-dilemma may have been inherited by methods that use the actual RAP-MUSIC. Contrary to these methods, our improvement is not an additional step, but a correction applied within the iterative MUSIC algorithm.

We compare TRAP-MUSIC with RAP-MUSIC, providing both illustrative examples and statistical evidence from extensive simulations with varying key parameters, *e.g.*, SNR, number of recursion steps and temporal correlation between sources. In addition, using reader-friendly basic linear algebra, we give a solid mathematical justification for the concepts on which TRAP-MUSIC is based, and demonstrate its performance on measured MEG data.

We argue that TRAP-MUSIC is an efficient and useful tool for revealing the active brain from MEG/EEG data. Its improvements in performance come without any computational cost, and thus, it is suitable for both online and offline applications (for online use of RAP-MUSIC, see *e.g.*, Dinh et al. (2012, 2014)). Essentially, TRAP-MUSIC should be suitable for any application where RAP-MUSIC could be considered, and it may open new windows for MUSIC in analysis of MEG/EEG.

Theory and methods

Description of the measurement data

We assume that the (noiseless part of the) measurement data are generated by a finite number of cortical sources that can be modeled by a set of equivalent current dipoles (Hämäläinen et al., 1993).

We denote a current dipole by a pair $(\mathbf{p}, \boldsymbol{\eta})$, where $\mathbf{p}$ is the location and the unit vector $\boldsymbol{\eta}$ is the orientation of the dipole. The amplitude of a dipole is denoted by s and so its dipole moment is $s\boldsymbol{\eta}$. For m sensors, the sensor-readings vector, or topography, due to a unit-strength source is denoted by $\mathbf{l}(\mathbf{p}, \boldsymbol{\eta})$.

To every dipole location $\mathbf{p}$ we assign a local lead-field matrix $\mathbf{L}(\mathbf{p})$ whose columns are $\mathbf{l}(\mathbf{p}, \mathbf{e}_x)$, $\mathbf{l}(\mathbf{p}, \mathbf{e}_y)$, and $\mathbf{l}(\mathbf{p}, \mathbf{e}_z)$, where the orientations $\mathbf{e}_x$, $\mathbf{e}_y$ and $\mathbf{e}_z$ are the Cartesian unit vectors. It follows that $\mathbf{l}(\mathbf{p}, \boldsymbol{\eta}) = \mathbf{L}(\mathbf{p})\,\boldsymbol{\eta}$.

We assume that the measurement data, collected in the data matrix $\mathbf{Y}$, is obtained at N time-points and is due to an unknown, finite number n of source dipoles and additive noise. The amplitudes s_{ij} of the sources $i = 1, \ldots, n$ at time points t_j, $j = 1, \ldots, N$ are collected in a time-course matrix $\mathbf{S}$, where row $\mathbf{s}_i$ of $\mathbf{S}$ is the time-course of source i.

The noisy measurement data collected by $m > n$ sensors is described by the linear model

$$\mathbf{Y} = \mathbf{Y}_0 + \boldsymbol{\varepsilon} = \mathbf{AS} + \boldsymbol{\varepsilon}, \tag{1}$$

where $\mathbf{A} = [\mathbf{l}(\mathbf{p}_1, \boldsymbol{\eta}_1), \ldots, \mathbf{l}(\mathbf{p}_n, \boldsymbol{\eta}_n)]$ is the mixing matrix, $\mathbf{Y}_0 = \mathbf{AS}$ the noiseless data matrix, and $\boldsymbol{\varepsilon}$ the noise matrix. The noise is assumed to be statistically independent of $\mathbf{A}$ and $\mathbf{S}$. We call the noise *white* if its (not-normalized) covariance matrix $\boldsymbol{\varepsilon}\boldsymbol{\varepsilon}^{\mathrm{T}}$ is $\alpha\mathbf{I}$ with $\alpha > 0$ and identity matrix $\mathbf{I}$; otherwise it is *colored*.

We assume that the columns of $\mathbf{A}$, $\mathbf{l}(\mathbf{p}_j, \boldsymbol{\eta}_j)$, are linearly independent, *i.e.*, $\mathrm{rank}(\mathbf{A}) = n$. Also, we assume that the time-courses $\mathbf{S}$ are time-centered, *i.e.*, have zero mean, and that they are non-vanishing and linearly independent, so that $\mathrm{rank}(\mathbf{S}) = n$. Note that the time-courses may be correlated, *i.e.*, $\mathbf{s}_i\,\mathbf{s}_j^{\mathrm{T}}$, where T denotes transpose, may be non-zero for $i \neq j$. Finally, we assume that a sufficiently accurate forward model is available.

MUSIC

The objective of MUSIC-type methods is to estimate the source parameters from the noisy measurement data $\mathbf{Y}$ (Mosher and Leahy, 1998, 1999; Schmidt, 1986) with the aid of spatial/physical information of the forward model and temporal information of the measured time-series signals. In other words, one wants to find the sources, typically dipoles $(\mathbf{p}_1, \boldsymbol{\eta}_1), \ldots, (\mathbf{p}_n, \boldsymbol{\eta}_n)$. In practice, localization is done by a localizer (function), which is evaluated at all source-location candidates in the discretized scanning grid overlaid on the ROI. The maxima of the localizer correspond to the estimated source locations. It is worth noticing that real sources are not point-like, and they are not exactly at the scanning grid points—neither in practice and nor in our simulations (Kaipio and Somersalo, 2007).

MUSIC algorithms are based on the separation of data space, span $(\mathbf{Y})$, into two mutually orthogonal subspaces, the *signal space* $\mathrm{span}(\mathbf{A})$ and the *noise space* $\mathrm{span}(\mathbf{A})^{\perp}$; $\mathrm{span}(\mathbf{Y})$ and $\mathrm{span}(\mathbf{A})$ refer to vector subspaces spanned by the columns of $\mathbf{Y}$ and $\mathbf{A}$, respectively. Let $\mathbf{P}_{\mathrm{sg}} = \mathbf{AA}^{\dagger}$, where $\dagger$ is the Moore–Penrose pseudoinverse, be the orthogonal projection from $\mathbb{R}^m$ data space onto $\mathrm{span}(\mathbf{A})$, *i.e.*, it is the projection to the brain-signal space.

MUSIC algorithms are usually divided into two categories: *scalar* MUSIC, which is used if the orientations of the test dipoles in the ROI are predetermined and fixed for each location in the forward model, and *vector* MUSIC if the dipole orientations are not predetermined or known *a priori* (Mosher and Leahy, 1999; Sekihara and Nagarajan, 2008; Hämäläinen et al., 1993). In the fixed-orientation case, the orientation $\boldsymbol{\eta}$ is a function of location $\mathbf{p}$, *i.e.*, $\boldsymbol{\eta} = \boldsymbol{\eta}(\mathbf{p})$; consequently, the topographies $\mathbf{l}(\mathbf{p}, \boldsymbol{\eta}) = \mathbf{L}(\mathbf{p})\boldsymbol{\eta}(\mathbf{p})$ are functions of only the location $\mathbf{p}$.

For simplicity, consider here scalar MUSIC. Scalar MUSIC is based on the following property of the signal-space projection $\mathbf{P}_{\mathrm{sg}}$: for any $\mathbf{p}$ in the ROI, $\mathbf{P}_{\mathrm{sg}}\mathbf{l}(\mathbf{p}) = \mathbf{l}(\mathbf{p})$ if $\mathbf{l}(\mathbf{p})$ is one of the actual source topographies that contributed to $\mathrm{span}(\mathbf{A})$, and $\|\mathbf{P}_{\mathrm{sg}}\mathbf{l}(\mathbf{p})\| < \|\mathbf{l}(\mathbf{p})\|$ otherwise; $\|\,.\,\|$ denotes the Euclidean norm $\|\mathbf{x}\|^2 = (|x_1|^2 + \ldots + |x_m|^2)^{1/2}$ for any m-vector $\mathbf{x}$.

Consider next the data equation Eq. (1) with white noise $\boldsymbol{\varepsilon}$, *i.e.*, $\boldsymbol{\varepsilon}\boldsymbol{\varepsilon}^{\mathrm{T}} = \sigma^2\mathbf{I}$. Given the covariance matrix of the data $\mathbf{C} = \mathbf{YY}^{\mathrm{T}}$, the separation to signal and noise spaces can be done by an eigenvalue decomposition of C as follows:

$$\mathbf{C} = \mathbf{C}_0 + \sigma^2\mathbf{I} = \mathbf{U}\,\mathrm{diag}_{m\times m}\left(d_1 + \sigma^2, \ldots, d_n + \sigma^2, \sigma^2, \ldots, \sigma^2\right)\mathbf{U}^{\mathrm{T}}, \tag{2}$$

where $\mathbf{C}_0 = \mathbf{UDU}^{\mathrm{T}}$ is the covariance matrix of the noiseless data, where $\mathbf{U}$ is an $m \times m$ orthonormal matrix, and $d_1 \geq \ldots \geq d_n > d_{n+1} = \ldots = d_m = 0$ are the diagonal elements of $\mathbf{D}$, and σ is the noise level. Let $\mathbf{U}_{\mathrm{sg}} = \mathbf{U}(:, 1:n)$. Here we use the Matlab notation, where $\mathbf{M}(i, :)$ and $\mathbf{M}(:, j)$ are the ith row and jth column of the matrix $\mathbf{M}$, respectively. Because, $\mathbf{C}_0 = \mathbf{UDU}^{\mathrm{T}}$, then $\mathrm{span}(\mathbf{U}_{\mathrm{sg}}) = \mathrm{span}(\mathbf{A})$, which is the signal space, and so the exact projection to the signal space is $\mathbf{P}_{\mathrm{sg}} = \mathbf{U}_{\mathrm{sg}}\mathbf{U}_{\mathrm{sg}}^{\mathrm{T}}$.

In practice, we do not know the true number n of the sources. In theory, we could estimate n from the eigenvalue decomposition of the data covariance matrix $\mathbf{C}$, by determining the index j after which the eigenvalues d_j drop and stay flat, representing noise. However, it is often hard or even impossible to see a clear, reliable drop or plateau in this eigenvalue spectrum, and hence, an overestimation of n has been recommended to ensure that the true signal space definitely belongs to the estimated signal space (Mosher and Leahy, 1999; Liu and Schimpf, 2006;

Moiseev et al., 2011). MUSIC algorithms are therefore initialized with $\tilde{n} > n$ in practice; this choice also determines the number of recursion steps. Let $\mathbf{U}_s = \mathbf{U}(:, 1:\tilde{n})$. Then, $\mathbf{P}_s = \mathbf{U}_s\mathbf{U}_s^T$, instead of $\mathbf{P}_{sg}$, can be used to identify the sources, similar to $\mathbf{P}_{sg}$. This is because span($\mathbf{P}_{sg}$) is a subspace of span($\mathbf{P}_s$) and the $\tilde{n} - n$ extra dimensions of span($\mathbf{P}_s$) represent only noise. Accordingly, the *localizer* for the scalar MUSIC is given by

$$\mu(\mathbf{p}) = \frac{\|\mathbf{P}_s\mathbf{l}(\mathbf{p})\|^2}{\|\mathbf{l}(\mathbf{p})\|^2}, \tag{3}$$

where $\mu(\mathbf{p}) \approx 1$ if $\mathbf{p}$ is one of the true sources at $\mathbf{p}_1, \ldots, \mathbf{p}_n$, and $\mu(\mathbf{p}) < 1$ if there is no source at (or near) $\mathbf{p}$. So, the source locations, corresponding to the n largest local maxima of $\mu(\mathbf{p})$, can in principle be found by computing $\mu(\mathbf{p})$ for each candidate-source location in the scanning grid.

If an estimate $\mathbf{C}_\varepsilon$ of the noise covariance is available, we can whiten the data equation (1) by multiplying its both sides with (a reasonably regularized) $\mathbf{C}_\varepsilon^{-1/2}$. In MEG and EEG, the noise estimate can be obtained, for example, from the pre-stimulus part of the signal; in MEG, an empty-room measurement could also be used to determine the measurement (sensor) noise. Therefore, unless otherwise stated, we assume that the data are either corrupted by (approximately) white noise, or the data have been whitened. We, however, note that given a sufficient SNR, MUSIC methods also work in practice to some extent with colored noise.

If the forward model does not contain any constraints on the source orientations, the vector MUSIC is used; its localizer $\mu(\mathbf{p})$ is given by

$$\mu(\mathbf{p}) = \max_{\|\boldsymbol{\eta}\|=1} \frac{\|\mathbf{P}_s\mathbf{L}(\mathbf{p})\boldsymbol{\eta}\|^2}{\|\mathbf{L}(\mathbf{p})\boldsymbol{\eta}\|^2}. \tag{4}$$

Because $\mathbf{l}(\mathbf{p}, \boldsymbol{\eta}) = \mathbf{L}(\mathbf{p})\boldsymbol{\eta}$ belongs to span($\mathbf{A}$) only for a true source at $\mathbf{p} = \mathbf{p}_k$ and $\boldsymbol{\eta} = \pm\boldsymbol{\eta}_k$ for some k, $1 \le k \le n$, we can reason that $\mu(\mathbf{p}) \approx 1$ if $\mathbf{p}$ is one of the true sources $\mathbf{p}_1, \ldots, \mathbf{p}_n$ and $\mu(\mathbf{p}) < 1$, otherwise. The orientations of the sources can be determined in closed form: the maxima $\mu(\mathbf{p})$ and maximizer $\boldsymbol{\eta}^{\text{vec}}$ of the expression in Eq. (4) are derived by making a change of variable $\mathbf{z} = \mathbf{F}^{-1}\boldsymbol{\eta}$ with $\mathbf{F} = (\mathbf{L}(\mathbf{p})^T\mathbf{L}(\mathbf{p}))^{-1/2}$, and observing that it turns the task to maximize a quadratic form $\mathbf{z}^T\mathbf{K}\mathbf{z}$ for $\|\mathbf{z}\| = 1$, with $\mathbf{K} = \mathbf{F}\mathbf{L}(\mathbf{p})^T\mathbf{P}_s\mathbf{L}(\mathbf{p})\mathbf{F}$. With $\boldsymbol{\eta}^{\text{vec}}(\mathbf{p})$, we can assign a topography $\mathbf{l}^{\text{vec}}(\mathbf{p}) = \mathbf{L}(\mathbf{p})\boldsymbol{\eta}^{\text{vec}}(\mathbf{p})$ to every $\mathbf{p}$ in the ROI. This transforms vector MUSIC to the scalar one with $\mathbf{l}(\mathbf{p})$ replaced by $\mathbf{l}^{\text{vec}}(\mathbf{p})$.

General concepts of recursive MUSIC algorithms

Here, we briefly introduce the basic concepts of recursive MUSIC, using as an example the conventional RAP-MUSIC, in which the sources are found one after another (Mosher and Leahy, 1999). At each recursion step, the topography of one source is projected out of the data and the forward model; the MUSIC algorithm is then applied to the transformed data equation. Essentially, RAP-MUSIC transforms the difficult problem of finding n local maxima of the localizer in one round into a much simpler problem of finding one global maximum at each sequential round.

The RAP-MUSIC process starts with a plain MUSIC scan step, which gives the estimate of the first source location $\hat{\mathbf{p}}_1$ as the global maximum point of the localizer $\mu(\mathbf{p})$. The topography $\hat{\mathbf{l}}_1$ at $\hat{\mathbf{p}}_1$ for scalar MUSIC is $\mathbf{l}(\hat{\mathbf{p}}_1)$, and for vector MUSIC, $\hat{\mathbf{l}}_1 = \mathbf{L}(\hat{\mathbf{p}}_1)\boldsymbol{\eta}^{\text{vec}}(\hat{\mathbf{p}}_1)$.

After source locations $\hat{\mathbf{p}}_1, \ldots, \hat{\mathbf{p}}_{k-1}$ with topographies $\hat{\mathbf{l}}_1, \ldots, \hat{\mathbf{l}}_{k-1}$ have been found, we find $\hat{\mathbf{p}}_k$ and $\hat{\mathbf{l}}_k$ in the kth recursion step as follows. We form an orthogonal projection, the *out-projector* $\mathbf{Q}_k$, by

$$\mathbf{Q}_k = \mathbf{I} - \mathbf{B}_k\mathbf{B}_k^\dagger, \tag{5}$$

where $\mathbf{B}_k = [\hat{\mathbf{l}}_1, \ldots, \hat{\mathbf{l}}_{k-1}]$ contains the topographies of the previously found sources. Then $0 = \mathbf{Q}_k\hat{\mathbf{l}}_j \simeq \mathbf{Q}_k\mathbf{l}_j$ for $j < k$. The transformed (approximated) signal space is span($\mathbf{Q}_k\mathbf{U}_s$). Next we form the singular value decomposition (SVD) of $\mathbf{Q}_k\mathbf{U}_s$ as $\mathbf{Q}_k\mathbf{U}_s = \mathbf{U}_k\mathbf{D}_k\mathbf{V}_k^T$, where $\mathbf{U}_k$ is an $m \times m$ orthonormal matrix, and the singular values $d_1 \ge \ldots \ge d_{\tilde{n}}$ are the diagonal elements of $\mathbf{D}_\mathbf{k}$. With this SVD, we can compute the orthogonal projection $\mathbf{P}_k$ onto span($\mathbf{Q}_k\mathbf{U}_s$) by

$$\mathbf{P}_k = \sum_{j=1}^{\tilde{n}} \mathbf{u}_{kj}\mathbf{u}_{kj}^T = \mathbf{U}_k(:, 1:\tilde{n})\mathbf{U}_k(:, 1:\tilde{n})^T, \tag{6}$$

where $\mathbf{u}_{kj} = \mathbf{U}_k(:, j)$ and $\tilde{n} \ge n$. For the kth recursion step, the scalar RAP-MUSIC localizer $\mu_k(\mathbf{p})$ is given by

$$\mu_k(\mathbf{p}) = \frac{\|\mathbf{P}_k\mathbf{Q}_k\mathbf{l}(\mathbf{p})\|^2}{\|\mathbf{Q}_k\mathbf{l}(\mathbf{p})\|^2}, \tag{7}$$

and the vector RAP-MUSIC localizer by

$$\mu_k(\mathbf{p}) = \max_{\|\boldsymbol{\eta}\|=1} \frac{\|\mathbf{P}_k\mathbf{Q}_k\mathbf{L}(\mathbf{p})\boldsymbol{\eta}\|^2}{\|\mathbf{Q}_k\mathbf{L}(\mathbf{p})\boldsymbol{\eta}\|^2}, \tag{8}$$

where the closed forms for $\mu_k(\mathbf{p})$ and its maximizer $\boldsymbol{\eta}_k^{\text{vec}}(\mathbf{p})$ are obtained with basic linear algebra, as explained in the previous section.

The location $\hat{\mathbf{p}}_k$ is now the global maximum point of the localizer $\mu_k(\mathbf{p})$. For the scalar RAP-MUSIC, the topography $\hat{\mathbf{l}}_k$ is given by $\hat{\mathbf{l}}_k = \mathbf{l}(\hat{\mathbf{p}}_k)$, and for the vector RAP-MUSIC, by $\hat{\mathbf{l}}_k = \mathbf{L}(\hat{\mathbf{p}}_k)\boldsymbol{\eta}_k^{\text{vec}}(\hat{\mathbf{p}}_k)$.

Note that at each recursive step, RAP-MUSIC (Mosher and Leahy, 1999) performs the same operation as the conventional MUSIC (Schmidt, 1986) but applied to the transformed data equation

$$\mathbf{Q}_k\mathbf{Y} = \mathbf{Q}_k\mathbf{A}\mathbf{S} + \mathbf{Q}_k\boldsymbol{\varepsilon}, \tag{9}$$

which has the same form as the original data equation Eq. (1) with the additional out-projector $\mathbf{Q}_k$ applied to the left and right sides.

The recursive process is continued until all sources have been found, which should be indicated by a significantly reduced maximum value of $\mu_k(\mathbf{p})$ after $k = n$ steps; a 'plateau' of low values should be observed in μ_k as function of k after n steps. The drop could then be used as a stopping rule or as a classifier separating n true and $\tilde{n} - n$ false sources for recursive MUSIC algorithms. Some fixed thresholds, *e.g.*, 0.95 or 0.8 for $\max\mu_k(\mathbf{p})$ have been suggested (Mosher and Leahy, 1999; Liu and Schimpf, 2006); using a fixed threshold has, however, been shown to be very sensitive, for example, to the SNR and to the configuration of the sources, and hence, adaptive techniques have been suggested (Katyal and Schimpf, 2004; Cheyne et al., 2006). The drop, leading to a plateau, does not, however, happen for RAP-MUSIC due to the RAP dilemma, as we show in the following section.

The RAP dilemma

The conventional RAP-MUSIC (Mosher and Leahy, 1999) has the unwanted property that in the recursive process, it leaves large residual values of the localizer $\mu_k(\mathbf{p})$, for example, in the vicinity of already-found sources. These residuals stem from preceding recursion steps due to imperfect out-projection of the true topographies that correspond to the already-found sources; this RAP dilemma can degrade source estimation in the subsequent rounds.

The origin of the RAP dilemma can be explained with the following reasoning, applied on the data equation (9) and the RAP-MUSIC localizer (7) (or (8)). From Eq. (2) we see that span($\mathbf{A}$) is a subspace of span($\mathbf{U}_s$). Consider the kth recursion step of RAP-MUSIC, where $\mathbf{l}_1, \ldots, \mathbf{l}_n$ are the true topographies of the sources, while $\hat{\mathbf{p}}_1, \ldots, \hat{\mathbf{p}}_{k-1}$ and $\hat{\mathbf{l}}_1, \ldots, \hat{\mathbf{l}}_{k-1}$ are the corresponding already-found locations and topographies with $\hat{\mathbf{l}}_j \simeq \mathbf{l}_j$ for $j < k$. Then $0 = \mathbf{Q}_k\hat{\mathbf{l}}_j \neq \mathbf{Q}_k\mathbf{l}_j$ because $\hat{\mathbf{l}}_j$ is not exactly equal to $\mathbf{l}_j$.

On the other hand, $\mathbf{l}_j$ belongs to the true signal space span($\mathbf{A}$), which is a subspace of span($\mathbf{U}_s$); thus, $\mathbf{Q}_k\mathbf{l}_j$ belongs to the kth signal space

estimate span($\mathbf{Q}_k\mathbf{U}_s$). This implies that $\mathbf{P}_k\mathbf{Q}_k\mathbf{l}_j = \mathbf{Q}_k\mathbf{l}_j$ with $\mathbf{P}_k$ as in Eq. (6), and so

$$\mu_k(\mathbf{p}_j) = \frac{\left\|\mathbf{P}_k\mathbf{Q}_k\mathbf{l}_j\right\|^2}{\left\|\mathbf{Q}_k\mathbf{l}_j\right\|^2} = 1 \tag{10}$$

for already-found sources. So, the maximum of $\mu_k(\mathbf{p})$ over $\mathbf{p}$ in the ROI is equal to 1 and it is attained at all locations $\mathbf{p}_j$, for $j<k$. This may lead to a wrong choice of $\widehat{\mathbf{p}}_k$, because $\mu_k(\mathbf{p})\simeq 1$ also in the neighborhoods of the locations $\mathbf{p}_j$, due to the continuity of $\mu_k(\mathbf{p})$. Note that the RAP dilemma exists even with the correct $\tilde{n} = n$.

In other words, the RAP-dilemma prevents RAP-MUSIC from cleaning out the source information of previous recursion steps. This may lead to spurious localizer maxima in the subsequent rounds. In particular, the RAP dilemma hinders RAP-MUSIC from correctly estimating the number of the sources. Fortunately, this issue can be overcome by using TRAP-MUSIC.

Truncated RAP-MUSIC (TRAP-MUSIC)

The core idea of TRAP-MUSIC is to apply a sequential dimension reduction of the estimated remaining signal space at each recursion step. The rationale for the sequential dimension reduction of the projection to the signal space is conceptually explained as follows. At each recursion step, one source is found and projected out, and hence, for the following step, there is one source less in the remaining signal space. In other words, after the kth step is completed, there are $n-k$ sources left to be found, and hence, it is reasonable to limit the dimension of the remaining signal space to $\tilde{n}-k$.

TRAP-MUSIC differs from the conventional RAP-MUSIC in the way it approximates the transformed signal subspace span($\mathbf{Q}_k\mathbf{A}$) at each recursion step. Analogously to RAP-MUSIC, we define the projection to the transformed signal subspace at the kth recursion as

$$\mathbf{P}_k^{\mathrm{TRAP}} = \sum_{j=1}^{\tilde{n}-(k-1)} \mathbf{u}_{kj}\mathbf{u}_{kj}^{\mathrm{T}} = \mathbf{U}_k(:, 1:\tilde{n}-(k-1))\mathbf{U}_k(:, 1:\tilde{n}-(k-1))^{\mathrm{T}}, \tag{11}$$

where $\mathbf{U}_k$ is as in Eq. (6) and the corresponding scalar scanning function is given by

$$\mu_k^{\mathrm{TRAP}}(\mathbf{p}) = \frac{\left\|\mathbf{P}_k^{\mathrm{TRAP}}\mathbf{Q}_k\mathbf{l}(\mathbf{p})\right\|^2}{\left\|\mathbf{Q}_k\mathbf{l}(\mathbf{p})\right\|^2}, \tag{12}$$

and the vector TRAP-MUSIC localizer by

$$\mu_k^{\mathrm{TRAP}}(\mathbf{p}) = \max_{\|\boldsymbol{\eta}\|=1} \frac{\left\|\mathbf{P}_k^{\mathrm{TRAP}}\mathbf{Q}_k\mathbf{L}(\mathbf{p})\boldsymbol{\eta}\right\|^2}{\left\|\mathbf{Q}_k\mathbf{L}(\mathbf{p})\boldsymbol{\eta}\right\|^2}. \tag{13}$$

The source orientations are determined as in RAP-MUSIC, but using $\mathbf{P}_k^{\mathrm{TRAP}}$ instead of $\mathbf{P}_k$. Next, we will explain why TRAP-MUSIC localizers are free from the RAP dilemma.

Removal of the RAP dilemma with TRAP-MUSIC

The removal of the RAP dilemma can be explained as follows. Let us first present the estimated signal space spanned by $\mathbf{U}_s = \mathbf{U}(:, 1:\tilde{n})$ as follows:

$$\mathrm{span}(\mathbf{U}_s) = \mathrm{span}([\mathbf{l}_1, \ldots, \mathbf{l}_n, \mathbf{w}_{n+1}, \ldots, \mathbf{w}_{\tilde{n}}]), \tag{14}$$

where $\mathbf{w}_j = \mathbf{U}_s(:, j)$, with $n+1 \le j \le \tilde{n}$, are those columns of $\mathbf{U}_s$ that are solely due to noise. Let us consider the kth recursion step, keeping in mind the SVD $\mathbf{Q}_k\mathbf{U}_s = \mathbf{U}_k\mathbf{D}_k\mathbf{V}_k^{\mathrm{T}}$, where the columns of $\mathbf{U}_k$ form an orthonormal basis of span($\mathbf{Q}_k\mathbf{U}_s$). We see that the estimated signal-subspace span($\mathbf{Q}_k\mathbf{U}_s$) = span($[\mathbf{Q}_k\mathbf{l}_1, \ldots, \mathbf{Q}_k\mathbf{l}_n, \mathbf{Q}_k\mathbf{w}_{n+1}, \ldots, \mathbf{Q}_k\mathbf{w}_{\tilde{n}}]$). The out-projector $\mathbf{Q}_k$ (Eq. (5)) makes the projections $\mathbf{Q}_k\mathbf{l}_j, j<k$, of the already-found topographies almost vanishing, while it affects the topographies $\mathbf{l}_k, \ldots, \mathbf{l}_n$ much less, given that the source topographies were originally linearly independent. Furthermore, assuming that the out-projection is nearly accurate, these small residuals $\mathbf{Q}_k\mathbf{l}_j, j<k$, are practically arbitrarily oriented. Thus, the power of the residual is relatively small and the residuals spread over all dimensions of span($\mathbf{Q}_k\mathbf{U}_s$). At each recursion step k, the dimension with the smallest singular value is due to the residuals, and consequently, removing this dimension from the signal space eliminates the possibility that a large localizer value is attained solely due to the residuals. TRAP-MUSIC applies exactly this procedure in the projection $\mathbf{P}_k^{\mathrm{TRAP}}$, and hence, removes the RAP dilemma.

Simulations

In this section, we describe the simulations that provide both illustrative examples and statistical evidence about the advantages of TRAP-MUSIC compared to RAP-MUSIC. The simulations and analysis of all data were done in Matlab (The Mathworks Inc., Natick, MA, USA).

The head model and the BEM solver

The simulations were done using a realistically shaped head geometry. We preprocessed and segmented the T1-weighted MRIs of a healthy subject (a 29-year-old right-handed male) with FreeSurfer (Fischl, 2012) and MNE software (Gramfort et al., 2014) to obtain the brain, skull, and scalp surfaces; the surfaces were decimated to 5120 triangles, smoothed and corrected for possible morphological flaws using iso2mesh Matlab library (Fang and Boas, 2009). The conductivities of the scalp and brain were set to 0.33 $(\Omega\mathrm{m})^{-1}$, and to 1/50th of that for the skull (Gonçalves et al., 2003; Dannhauer et al., 2011). The 'true' source grid (*i.e.*, the ROI) was a 2-D axial lattice at the depth of 4 cm from the top of the head (for similar approach, see (Moiseev et al., 2011)). It had a 2.8-mm spacing between neighboring source locations. The simulated sources were semi-randomly selected from the source grid so that they were at least 3 cm from each other and at least 4 cm away from the center of the ROI. The source dipoles were oriented along the z axis, *i.e.*, upwards. The scanning grid with a spacing of 2 mm was overlaid on the ROI so that the source points and scanning grid points did not coincide. 60 EEG electrodes and 306 MEG sensors were simulated and co-registered with the head model to represent realistic measurement settings. Finally, we computed the lead fields with a boundary-element method based on linear Galerkin boundary elements, formulated with the isolated-source approach (Hämäläinen and Sarvas, 1989; Stenroos and Sarvas, 2012). We applied the vector forms of the MUSIC algorithms in all analyses. The head model is visualized in Fig. 1. White noise was added to the simulated brain signals in Simulations 1–3. Due to the different domains of the magnetometers and gradiometers, magnetometer noise

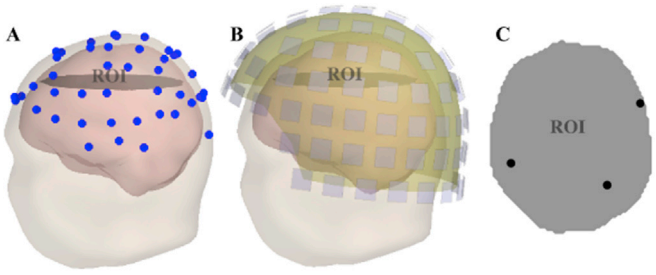

Fig. 1. The head model used in simulations, with **(A)** 60 EEG and **(B)** 306 MEG sensors (102 units consisting of one planar magnetometer and two gradiometers), and **(C)** the 2-D axial ROI with an example set of 3 sources. The ROI visualization in **(C)** is from above, and left-hand side is on the left.

was multiplied by a factor of 10 to obtain approximately even scaling for SNR in different sensors.

Simulation 1: comparison of RAP-MUSIC vs. TRAP-MUSIC in an example case

Here we demonstrated the performance of TRAP-MUSIC vs. RAP-MUSIC in an example case of simulated MEG data. The task was to evaluate (1) how well the methods can estimate the number of sources and (2) how accurately the sources are located.

In this simulation, $n = 3$ and $\tilde{n} = 6$ for both methods. The time courses were mixtures of sinusoids (between 10 and 30 Hz) and their mutual correlations ranged from 0.1 to 0.3. The analysis time window was 1 s. The SNR of the data was set to 5, computed as the ratio of the Frobenius norms of the noiseless data and noise matrices. We also repeated this simulation with uncorrelated sinusoidal time-courses for comparison.

We used an adaptive approach to obtain a contrast marker between true and false sources. We computed the difference between the maximum localizer values in successive recursions; the largest drop in this marker was used to estimate the number of sources. Geometrically this corresponds to a 'kink' in the graph of $\max_{\mathbf{p}} \mu_k(\mathbf{p})$ as function of k. We used this criterion in all simulations and in the analysis of measured data.

Simulation 2: estimating the number of the sources

We compared the ability of RAP- and TRAP-MUSIC to estimate the number and locations of the sources from a large set of simulated data with different properties.

With $n = 3$, $\tilde{n}$ was varied from $n + 1$ to $n + 6$. For each $\tilde{n}$, 100 MEG and 100 EEG data sets were simulated for SNRs of 10, 2, 1, 0.9, 0.5, and 0.33. Source time-courses were modeled as in Simulation 1. Simulations were repeated also for uncorrelated sources. The statistical significance of the comparison results was evaluated with Mann–Whitney U-tests with a significance level of 0.001 for a single comparison.

Simulation 3: residual sizes of RAP- and TRAP-MUSIC

We demonstrated the severity of the RAP dilemma by showing that the residuals are generated according to the theory introduced in Theory and Methods. This was done by computing the RAP-MUSIC localizer value according to Eq. (8) for the second recursion step at the exact location $\mathbf{p}_1$ of the source that was found at the first recursion step. That is, given the first source estimate $(\hat{\mathbf{p}}_1, \hat{\boldsymbol{\eta}}_1)$, we computed the out-projection $\mathbf{Q}_2$ and the signal-space projection $\mathbf{P}_2$ for the localizer, and computed it at the true source location $\mathbf{p}_1$, *i.e.*, $\mu_2(\mathbf{p}_1)$. To ensure that the recursive process actually removes the signals generated by the source at $\mathbf{p}_1$, $\mu_2(\mathbf{p}_1)$ should ideally be close to zero and in practice significantly smaller than 1. Values close to one would imply that signals due to previously found sources are left to the transformed data equation Eq. (9), which could hinder source estimation in subsequent recursions. Therefore, the value $\mu_2(\mathbf{p}_1)$ can be considered as the 'revisit residual' of the first source left at $\mathbf{p}_1$ at the second recursion. We also computed $\mu_2(\mathbf{p}_1)$ for TRAP-MUSIC (according to Eq. (13)), predicting that this value would be significantly smaller than for RAP-MUSIC. Note that because the localizer value is a continuous function of location, high localizer values are also present in the vicinity of the already-found sources; this phenomenon is confirmed in Simulation 1.

The revisit residual at the recursion step 2 of the source at $\mathbf{p}_1$ was defined as

$$\mu_2(\mathbf{p}_1) = \max_{\|\boldsymbol{\eta}\|=1} \frac{\|\mathbf{P}_2\mathbf{Q}_2\mathbf{L}(\mathbf{p}_1)\boldsymbol{\eta}\|^2}{\|\mathbf{Q}_2\mathbf{L}(\mathbf{p}_1)\boldsymbol{\eta}\|^2}, \tag{15}$$

where $\mathbf{Q}_2 = \mathbf{I} - \mathbf{B}_2\mathbf{B}_2^{\dagger} = \mathbf{I} - \left\|\hat{\mathbf{l}}_1\right\|^{-2}\hat{\mathbf{l}}_1\hat{\mathbf{l}}_1^{\mathrm{T}}$, $\mathbf{B}_2 = \hat{\mathbf{l}}_1 = \mathbf{L}(\hat{\mathbf{p}}_1)\hat{\boldsymbol{\eta}}_1$, and $\mathbf{P}_2$ is computed according to Eq. (6) for RAP-MUSIC and according to Eq. (11) for TRAP-MUSIC. The point in the scanning grid closest to the true source

The locations and the uncorrelated time-courses of $n = 3$ sources were modeled as in Simulations 1 and 2. The residual $\mu_2(\mathbf{p}_1)$ was computed for 1000 simulated EEG and 1000 simulated MEG data sets with SNRs of 10, 1, and 0.33. These simulations were performed for $\tilde{n} = 3$ and $\tilde{n} = 5$.

Measured MEG data

We carried out an MEG experiment using multimodal sensory stimuli. The MEG data were obtained from the same subject who was used for creating the head model geometry in Simulations 1–3. The subject gave a written informed consent. The experiments were performed in accordance with the Declaration of Helsinki, and they were approved by the Research Ethics Committee of Aalto University.

The subject was presented with unilateral somatosensory or visual stimuli. Electrical stimulation of the right or left median nerve was used as the somatosensory input and flashes of black-and-white chessboard patterns to the lower right or lower left visual field as the visual input. These stimuli are well-established and their (primary) brain responses are known to be located in the contralateral somatosensory or visual cortices, respectively (*e.g.*, Ahlfors et al. (1992); Mauguiere et al. (1997); Nakamura et al. (1998); Sharon et al. (2007)). The electrical stimulation consisted of 0.2-ms rectangular pulses, delivered with an intensity slightly below the motor threshold. The visual stimuli were presented for 100 ms exclusively in left or right lower visual field at a time; they were projected on a flat screen located at a distance of 100 cm from the subject.

The data were acquired with a 306-channel MEG scanner (Elekta Neuromag, Helsinki, Finland) located in the Aalto Neuroimaging MEG Core in Espoo, Finland, with a sampling frequency of 1000 Hz. For each stimulus type, 160 epochs were recorded in a randomized order with an inter-stimulus interval of 2.6–3 s.

The data were bandpass-filtered offline to 2–80 Hz. Data for each stimulus type were averaged over the epochs after a quality check of channels and epochs. An analysis window of 10–100 ms with respect to the stimulus triggers (at time $t = 0$) was used for the somatosensory data (the electrical stimulus artifact was excluded); a time window of 0–90 ms was used for the visual data. The time windows were equally long to allow mixing these data. The basic Maxfilter pipeline, including signal-space separation (Taulu et al., 2004) and interpolation of bad channels, was applied to the data with the Maxfilter software (Elekta Neuromag). As noted earlier, MUSIC is rather robust with respect to colored noise, and thus we chose to not whiten the data.

We used a realistic cortex geometry to analyze measured MEG data. The cortex model was computed from the subject's MRIs using Freesurfer and MNE software. The anatomical cortex model was reconstructed with a grid spacing of approximately 3.1 mm, resulting in 10242 grid points per hemisphere. The lead fields for the anatomical cortex model were computed without orientation constraint for the sources, using the same methodology as in The head model and the BEM solver.

In total, we analyzed 4 MEG data sets involving single sensory modality and 4 data sets generated by mixing the two modalities. The single-modality data were recorded during right or left median nerve stimulation (RSS; LSS), or by right or left visual-field (RVF; LVF) stimulation. The mixed data sets were produced by summing data from RSS, LSS, RVF, and LVF conditions. These mixed data sets to be analyzed were RSS + RVF, RSS + LVF, LSS + RVF, and LSS + LVF. The number of sources were estimated adaptively as in Simulations 1–3.

Results

Simulations

Simulation 1: comparison of TRAP-MUSIC and RAP-MUSIC in an example case

The localization and n-estimation results for the example case are

shown in Fig. 2. TRAP-MUSIC located all 3 sources accurately and estimated their number correctly. TRAP-MUSIC gave a high contrast between the 'true' and 'false' sources, *i.e.*, between the maximum localizer values of the recursion steps 1–3 and 4–6 (see Fig. 2). In steps 1–3, high localizer values indicated clearly the locations of the true sources; when a source was found, its topography was effectively cleaned from the subsequent rounds. This made locating the remaining sources easier and estimating the number of the sources clearer for both the algorithm and visual inspection.

On the other hand, while RAP-MUSIC also located the 3 true sources accurately, it completely failed in estimating the number of the sources. High localizer values were left to the neighborhoods of the already-found sources, making the subsequent localizer values misleading. Therefore, false positives occurred. The difference between the results with mildly correlated and uncorrelated time-courses was negligible.

Simulation 2: TRAP-MUSIC accurately estimates the number of sources

The success rates for estimating the number n of true sources and mean source localization errors for RAP-MUSIC and TRAP-MUSIC are shown in Fig. 3 for EEG and MEG data sets with $\tilde{n} = n+1, \ldots, n+6$ and SNRs of 10, 5, 2, 1, 0.9, 0.5, and 0.33 in the case of mildly correlated sources. Results were similar with fully uncorrelated sources.

For the EEG data sets, TRAP-MUSIC had a 100 % success rate for all $\tilde{n}$ and SNR conditions except for SNR = 0.33, whereas the success rates of RAP-MUSIC were always worse, and strongly dependent on the difference $\tilde{n} - n$; with even a small overestimation, RAP-MUSIC failed completely to give the correct number of sources. There were no significant differences in the mean source localization errors for any $\tilde{n}$ values between the methods, and the errors increased for both methods when the SNR decreased. The mean localization error was roughly 10 times larger with the lowest compared to the highest SNR. Also TRAP-MUSIC started to flounder in estimating n with the very low SNR of 0.33, which gave an approximate limit for the capability of the methods in our simulation setting.

For the simulated MEG data sets, TRAP-MUSIC had (almost) 100 % success rate independent of $\tilde{n} - n$ with all tested SNRs. With high SNRs, RAP-MUSIC had an equally good success rate only in the case of $\tilde{n} = n+1$, and the success rate decreased fast as function of $\tilde{n} - n > 1$. With lower SNRs, the difference of success rates between RAP- and TRAP-MUSIC became smaller and eventually disappeared.

RAP-MUSIC was not able to correctly estimate n in most situations, whereas TRAP-MUSIC gave a robust and correct estimate with high success rate, independent on the initial estimate $\tilde{n}$.

The maximum localizer value $\max_{\mathbf{p}} \mu_k(\mathbf{p})$ as function of the recursion step k is shown in Fig. 4 for both EEG and MEG with different $\tilde{n}$ and with SNR = 1. When the number of the recursion step k has reached the true number of sources (here, $n = 3$), the localizer value should drop drastically. This did not happen for RAP-MUSIC, for which the 'plateau' was observed in EEG systematically later than at the step $k = 3 = n$, and not at all for MEG. For TRAP-MUSIC, the largest drop of the localizer value was observed immediately after $n = 3$, giving a strong contrast between true and false sources at the correct index (Fig. 4).

Simulation 3: TRAP-MUSIC yields smaller residuals than RAP-MUSIC

Here we demonstrated the 'revisit residual', *i.e.*, the high localizer values at $\mathbf{p}_1$ at the recursion 2, given by Eq. (15). The mean residual sizes from 1000 simulations for RAP-MUSIC and TRAP-MUSIC are shown in Fig. 5. RAP-MUSIC behaved as predicted by the RAP dilemma; it left large residuals, whereas TRAP-MUSIC was able to project out (most of) the information related to the already-found topography, leaving only small residuals to the localizer. Results were similar with $\tilde{n} = n$ and $\tilde{n} = n+2$.

Measured MEG data

We applied TRAP-MUSIC on MEG data acquired during right/left somatosensory (RSS; LSS) or lower visual field (RVF; LVF) stimulation. Four recursive steps were carried out in TRAP-MUSIC for all analyzed data sets, *i.e.*, $\tilde{n} = 4$. The source localization results for the single-modality sensory stimuli are shown in Fig. 6. The primary responses were localized by TRAP-MUSIC to the left somatosensory cortex for RSS, to the right somatosensory cortex for LSS, to the left visual cortex for RVF, and to the right visual cortex for LVF (see Fig. 6). SNR was between 1.5 and 2.4 in all measured data sets, determined as the ratio of Frobenius norms of the data matrix of the analysis time-window and the −100… −10 ms pre-stimulus noise matrix.

In addition to the single-modality data, TRAP-MUSIC was applied also to the mixed multimodal sensory data for stimulus combinations RSS + RVF, RSS + LVF, LSS + RVF, and LSS + LVF. The localization results are shown in Fig. 7. TRAP-MUSIC was able to separate the somatosensory and visually evoked signals and locate them to their functionally representative cortical areas, matching well with the activated areas due to single modality stimulation cases, shown in Fig. 6. The

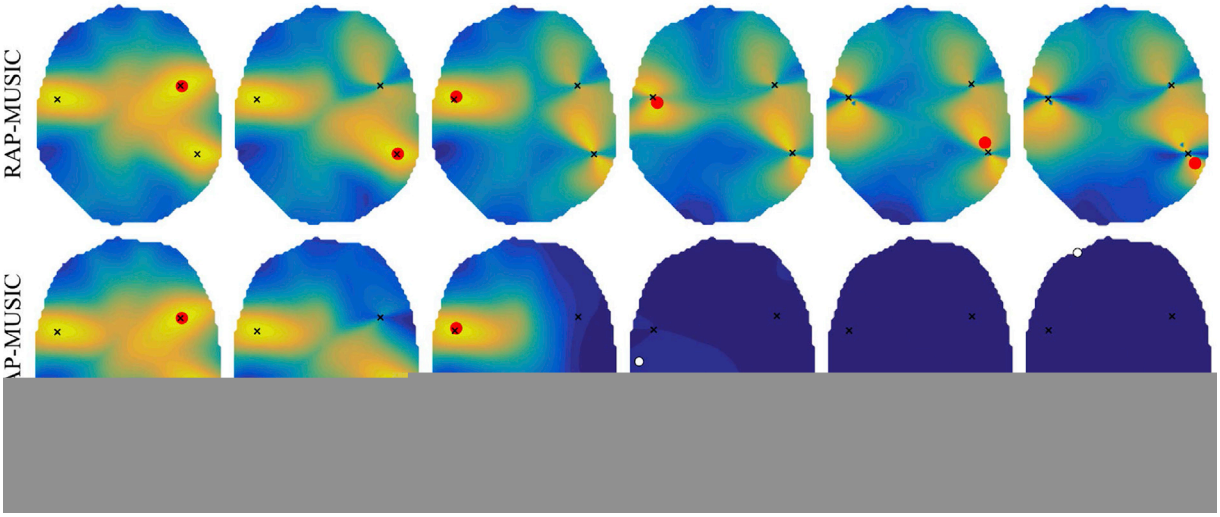

Fig. 2. Localization results of RAP-MUSIC vs. TRAP-MUSIC from a simulated MEG data with $n = 3$ sources. The localizer values for each recursion step are visualized with a colormap on the ROI. True sources are marked with black crosses. RAP-MUSIC failed to distinguish between the true and false sources. The residuals blurred the vicinity of the already-found sources, making both automatic and visual interpretation of the scanning results difficult. TRAP-MUSIC successfully found all 3 sources and did not suggest extra ones; it gave a high contrast between the true and false sources. Both methods found the true sources equally well. Localizer maxima classified as 'source' or 'no source' by the algorithms are marked with red and white dots, respectively.

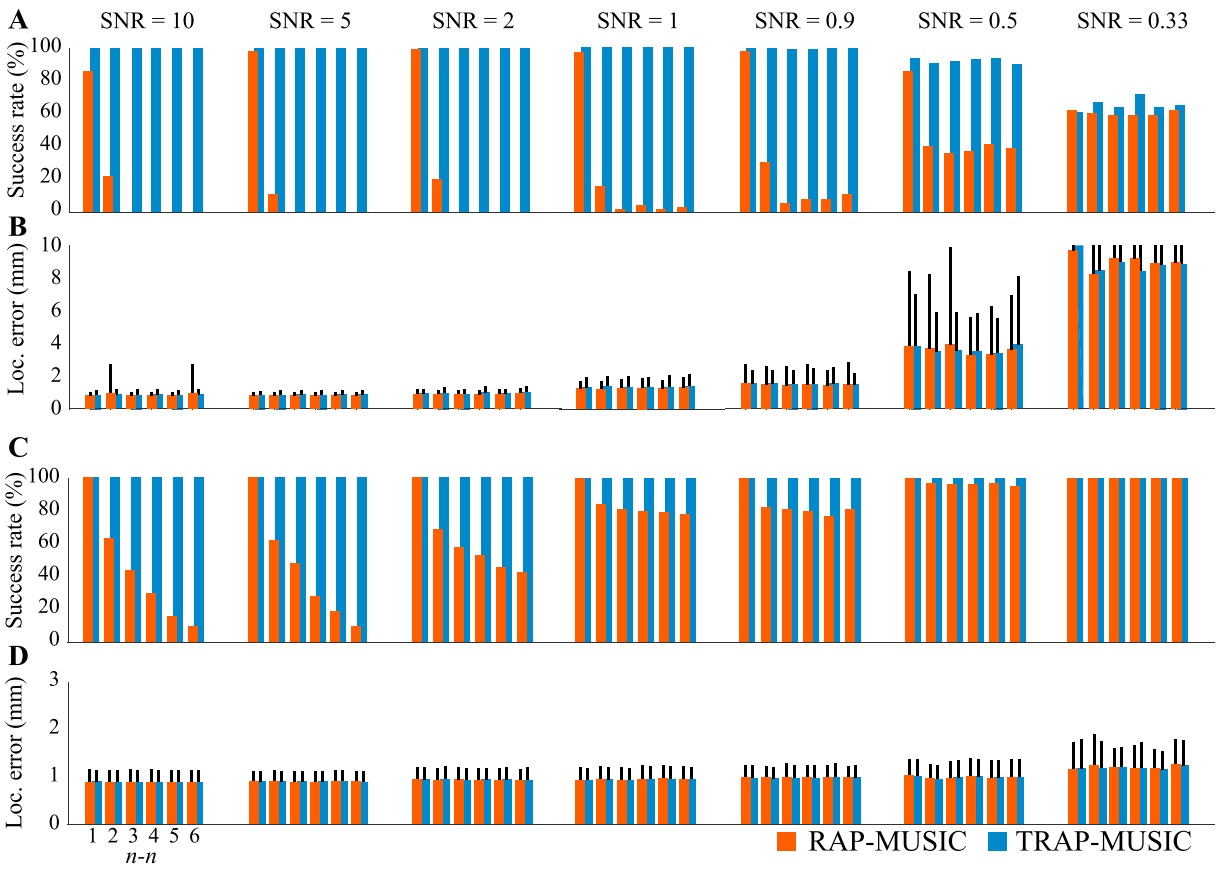

Fig. 3. Success rates for estimating the number of sources, and mean source localization errors as functions of $\tilde{n} - n$ with several SNRs for simulated EEG (**A** and **B**) and MEG (**C** and **D**) data for RAP- (orange) and TRAP-MUSIC (blue). Note that the black error bars in **(B)** for the SNR = 0.33 were partially cropped out. This was done to keep the scaling over SNR conditions fixed but visually reasonable; the error bars of the SNR = 0.33 were trivial, as for that SNR, both methods essentially failed in localizing the sources in EEG.

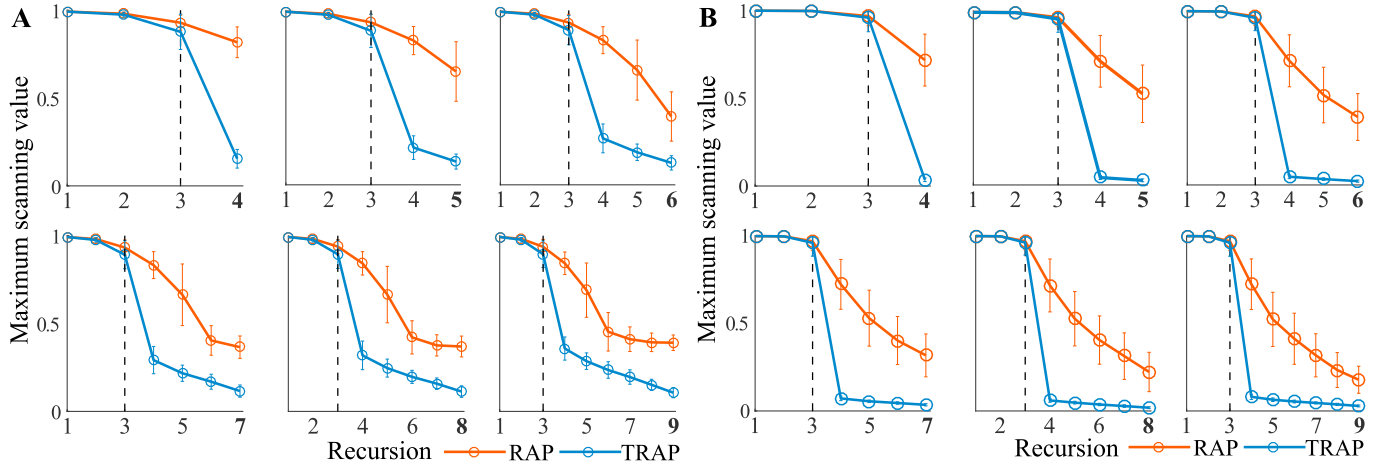

Fig. 4. The maximum value of the localizer $\mu_k(\mathbf{p})$ as function of the recursion step k for various values of $\tilde{n}$ plotted for RAP- (orange) and TRAP-MUSIC (blue) in EEG **(A)** and MEG **(B)** with SNR = 1 and $n = 3$. The curves are averages over 1000 data sets, and the error bars show the standard deviations. For TRAP-MUSIC, $\max_{\mathbf{p}} \mu_k(\mathbf{p})$ dropped dramatically after the nth step. This did not happen with RAP-MUSIC.

estimates for the number of sources were 2 for RSS + RVF, 3 for RSS + LVF, 3 for LSS + RVF, and 2 for LSS + LVF.

For the sources classified as 'true' by the TRAP-MUSIC, RAP-MUSIC yielded visually equal localization results, and had the same separation index for true and false sources as TRAP-MUSIC when 4 recursions were carried out. After these 'likely true' sources, the methods gave somewhat different results, and the maximum value of the localizer for TRAP-MUSIC seemed to decrease earlier and steeper than that of RAP-MUSIC (see Fig. 8), especially when the number of recursions was large (with $\tilde{n} = 6$ or 8).

Discussion

We analyzed the RAP dilemma and solved it by introducing a novel source localization method, TRAP-MUSIC. With 'RAP dilemma', we refer to the property of the original RAP-MUSIC that prevents it from

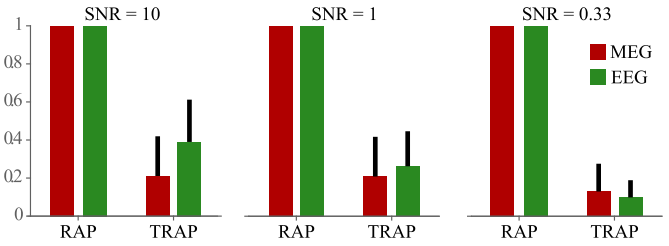

Fig. 5. Mean revisit residuals $\mu_2(\mathbf{p}_1)$, averaged over 1000 data sets with $n = 3$, presented for RAP-MUSIC and TRAP-MUSIC, for MEG (red) and EEG (green) data with SNRs of 10, 1, and 0.33. RAP-MUSIC left very high—actually maximal—residuals in the localizer value $\mu_2(\mathbf{p}_1)$, as predicted by the RAP dilemma, whereas TRAP-MUSIC had only small residuals.

completely removing the topographies of the already-found sources, yielding large residuals to subsequent recursion steps, which hinders the performance of the method. We showed that the RAP dilemma can be overcome by a sequential dimension reduction of the signal-space projection. By simulations, we showed that TRAP-MUSIC is significantly more accurate and robust in estimating the number of brain-signal sources than RAP-MUSIC. When we applied TRAP-MUSIC to measured MEG data, it located sources to their well-known functional representation areas in the cortex for data evoked by both single sensory input (*e.g.*, hand stimulus) and by multiple (*e.g.*, hand + visual stimulus) sensory inputs.

The original RAP-MUSIC holds potential as a simple and efficient source localization method, exploiting both the spatial and time domains to solve the inverse problem. It showed, however, to have a hidden deficiency preventing optimal performance. One potential reason for this deficiency remaining undiscovered thus far is that using identical grids and identical forward models for creating and scanning sources in simulations makes the RAP-dilemma disappear. It seems that Mosher and Leahy (1999) may have used identical grids for simulating and estimating sources. We also tested the performance of RAP-MUSIC using a simulation setting with identical grids; indeed, RAP-MUSIC was then able to reliably separate the true and false sources, with a contrast almost as good as that of TRAP-MUSIC. Nevertheless, using identical grids is an inverse crime and yields unrealistic, biased simulations (Kaipio and Somersalo, 2007).

Some recently introduced recursive MUSIC algorithms use the conventional RAP-MUSIC as a starting point and introduce improvements as additional steps (Liu and Schimpf, 2006; Ewald et al., 2014; Shahbazi et al., 2015). Our improvement, however, is not implemented by adding it *on top* of the already existing method; instead, it corrects a technically small but crucial deficiency *hidden within* the original RAP-MUSIC, allowing more reliable and robust source estimation. It may be possible that some issues of the RAP-dilemma area inherited by methods that use it as a starting point.

In Simulation 1, we demonstrated with simulated MEG data how RAP-MUSIC was unable to separate the true and false sources (see Fig. 2). The out-projection of the information related to the already-found sources was incomplete, and it left high localizer values in the vicinity of the already-found sources in the subsequent recursions. This made the localizer value distributions misleading, and hence, separating true and false sources by automatic classification or by visual inspection practically impossible. RAP-MUSIC often gave false positives, *i.e.*, had a poor positive predictive value. On the other hand, TRAP-MUSIC successfully found the true and only the true sources. TRAP-MUSIC effectively 'wipes out' the information related to preceding source estimates, and thus ensures that subsequent rounds are free from the residual artifacts. It is worth noticing that the unwanted residuals due to RAP-MUSIC appear not only in the vicinity of the estimated sources, but also several

Fig. 6. Localization results of the measured sensory-evoked MEG data for the single-modality data analyzed with TRAP-MUSIC. Four datasets with either right/left somatosensory or visual-field stimulation (RSS; LSS; RVF; LVF) were analyzed. Four recursion ($k = 1, \ldots, 4$) were carried out for each data set. The localizer values above 0.75 are visualized with a 'hot' colormap, and the localizer maxima for each recursion are marked with black dots. Note that the inflated cortices are shown either from axial or coronal orientation.

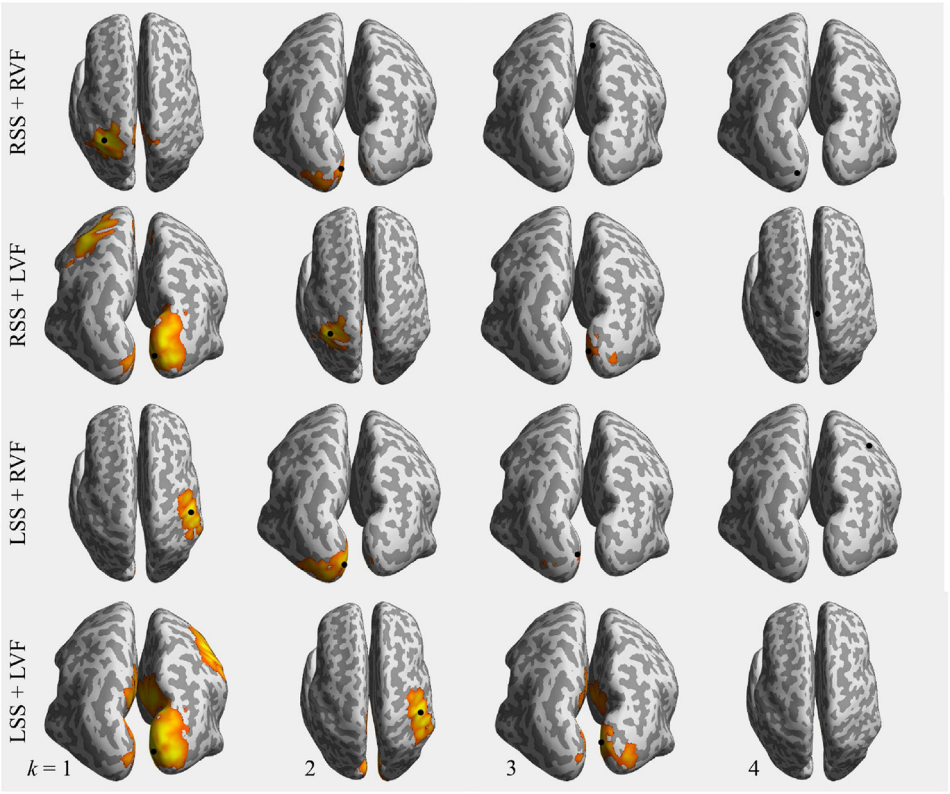

Fig. 7. TRAP-MUSIC localization results of the multisensory-evoked MEG data for the mixed modalities of right/left somatosensory (SS) + right/left visual-field (VF) stimulation: RSS + RVF, RSS + LVF, LSS + RVF, LSS + LVF. Four recursions ($k = 1, \ldots, 4$) were carried out for each data set. The localizer values above 0.75 are visualized with a 'hot' colormap, and the localizer maxima for each recursion are marked with black dots. Note that the inflated cortices are shown either from axial or coronal orientation.

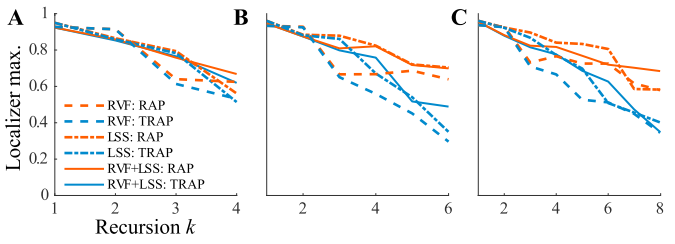

Fig. 8. The maximum value of the localizer as function of the recursion step for RAP-MUSIC (orange) and TRAP-MUSIC (blue) for three real MEG data sets: **(A)** right-visual field (RVF; dashed line), **(B)** left somatosensory (LSS; dotted dashed line), and **(C)** RVF + LSS (solid line). Both methods found the primary responses at their presumed cortical areas (see Fig. 6 and 7.) with highest localizer values.

centimeters away from them. TRAP-MUSIC could be particularly useful in applications with poor spatial resolution, *e.g.*, in (online) EEG applications that use only a small number of electrodes.

In Simulation 2, we compared RAP- and TRAP-MUSIC in a wide range of different source configurations, SNRs, and numbers of recursions in EEG and MEG. The results showed that the success rates in estimating n were high in almost all tested SNRs and values of $\tilde{n}$ for TRAP-MUSIC, whereas RAP-MUSIC failed drastically in evaluating n for almost all SNRs and $\tilde{n}$. The advantages of TRAP-MUSIC were most pronounced with moderate to high SNRs that are often available with evoked (and averaged) data. TRAP-MUSIC outperformed RAP-MUSIC in estimating n in both EEG and MEG, while keeping the localization accuracy of the true sources similar to that of RAP-MUSIC. With the lowest SNRs, the success-rate differences in the estimation of n became smaller, although TRAP-MUSIC was still better in most cases and never worse than RAP-MUSIC. Evidently, TRAP-MUSIC is able to perform well in a wide range of SNRs.

In Simulation 2, we also studied the evolution of the maximum localizer value as function of the recursion step k (Fig. 4). It was evident that the TRAP-MUSIC localizer value dropped when the true number of sources had been found, *i.e*, after $k = n$ steps (see Fig. 4), whereas the drop was observed later—if at all—for RAP-MUSIC. Thus, TRAP-MUSIC gave a strong contrast between the true and false sources and RAP-MUSIC did not. This illustrates the reason why the success rates of TRAP-MUSIC were so much higher than those of RAP-MUSIC.

The residuals predicted by the RAP dilemma were very pronounced in the idealistic cases of Simulation 3; RAP-MUSIC gave large—actually maximal—localizer values, *i.e.*, revisit residuals $\mu_2(\mathbf{p}_1) = 1$, when that value should have been $\ll 1$ (see Simulation 3 and Fig. 5 for details). On the other hand, TRAP-MUSIC yielded small residuals, suggesting that in subsequent rounds, the already-found sources should not affect the estimation of the remaining sources. It follows that the recursive global-maximum search is more likely to proceed to a new source point, and eventually, give very low localizer values indicating that all sources have been found. Note that as the localizer of RAP-MUSIC (and TRAP-MUSIC) is a continuous function of location, the residuals are not only present at the true source position, but also in the vicinity (see Fig. 2).

In practice, it is often impossible to know the true number n of the dominating sources that generate the data. Therefore, one needs to ensure that *at least* n recursions are run (*i.e.*, $\tilde{n} > n$) to ensure that the dimension of the applied signal space is at least as large as that of the true signal space (see Methods or, *e.g.*, Mosher and Leahy (1999)). Thus, there is always a need for separating 'true' and 'false' source estimates. The key factor in the performance of TRAP-MUSIC is its ability to do that separation. With TRAP-MUSIC, it should be safe to give a large $\tilde{n}$ at the initialization step of the algorithm, as it gives a robust and clear contrast between true and false positives. Note that setting the threshold for the separation of 'true' and 'false' sources can be done either with a fixed threshold value or adaptively. We used an adaptive approach, because a fixed threshold, for example $\mu = 0.95$ or 0.8 for separating the true and false sources, has been shown to be insufficient, and a generally suitable

threshold value cannot be used for data with, *e.g.*, different SNRs or with different source and sensor configurations (Katyal and Schimpf, 2004; Cheyne et al., 2006; Liu and Schimpf, 2006).

In this study, we used a fixed number of three true sources in the simulations. This was done for simplicity, to keep the parameter space reasonably limited. However, given a sufficient signal quality, TRAP-MUSIC can be used to locate a larger number of sources. We evaluated the performance of TRAP-MUSIC with several different values of n in the range 5–12, and the results were qualitatively very similar. We roughly evaluated the maximum number of sources that could be successfully located in our simulation setting in the case of SNR = 1; the tentative estimates were $n = 7$ for EEG and $n = 9$ for MEG.

To validate our TRAP-MUSIC algorithm, we used it to analyze measured MEG data evoked by stimulation of the right/left median nerve or right/left lower visual field. TRAP-MUSIC successfully located the primary responses to their well-known functional representation areas, *i.e.*, to the contralateral somatosensory cortex for median nerve stimulation and to contralateral visual cortex for visual-field stimulation. TRAP-MUSIC did not suggest additional spurious sources outside these areas, and the scanning function values dropped quickly after two or three recursions for each condition (see Fig. 6). This shows that TRAP-MUSIC is suitable for source analysis from typical sensory evoked MEG data. In addition, we used TRAP-MUSIC to locate sources from multisensory-evoked MEG. TRAP-MUSIC successfully separated and located brain activity from artificially mixed somatosensory- and visually-evoked data (Fig. 7). This suggests that TRAP-MUSIC indeed has the ability to separate brain activity related to different functional processes, that is, it works as a MUltiple SIgnal Classifier.

We also compared TRAP-MUSIC with RAP-MUSIC in the analysis of measured MEG data. Both methods located the primary responses to their corresponding functional areas from both single and mixed sensory modality data, giving essentially equal results for those few first responses. After the (primary) responses were located as expected at visual and/or somatosensory cortices, the methods showed different (possibly false) sources. In general, the maximal localizer value for TRAP-MUSIC decreased faster and steeper than for RAP-MUSIC (see Fig. 8), although the cut-off index was not as clearly visible as in Simulation 2 (see Fig. 4). As both the theory and our simulations suggest, RAP-MUSIC and TRAP-MUSIC should locate the true sources equally well. Therefore, one could possibly enhance the reliability of a MUSIC scan by applying both RAP-MUSIC and TRAP-MUSIC, and accept sources that both methods classified as sources. That is, take the estimate of the number of sources to be the recursion step index where the two methods diverge. These tentative suggestions need, however, further study.

TRAP-MUSIC is computationally efficient, similarly to RAP-MUSIC (Mosher and Leahy, 1999). RAP-MUSIC has already been used in real-time applications (Dinh et al., 2012, 2014). As the improvement of TRAP-MUSIC comes without any computational cost, it should be useful in online applications as well. In our simulations performed with a normal PC, a vector TRAP-MUSIC run took some fractions of a second, e.g., 0.1–0.9 s, depending on parameters such as the scanning grid size, number of recursions and the number of time-points. It is possible to further speed up the performance of TRAP-MUSIC, for example, by using its scalar version (in Eq. (12)), by applying optimum orientations (Vrba and Robinson, 2000; Sekihara and Nagarajan, 2008), or by scanning with fewer, regionally clustered lead fields (Dinh et al., 2015). Such optimization would allow the use of TRAP-MUSIC in real-time applications, such as closed-loop EEG systems.

It is worth noticing that the form of the time-courses (*e.g.*, whether they are sinusoidal, transient or random noise) does not affect the performance of MUSIC algorithms *per se*. The actual main input of MUSIC algorithms is the data covariance matrix, and the time-sample order could be changed without changing the localization result at all. However, the source time-courses affect the localization results in the way that if the time-courses are linearly dependent or correlated, this influences the covariance matrix. We briefly tested the performance of RAP- and TRAP-MUSIC with MEG with highly correlated (correlations between 0.7 and 0.9) and synchronous sources; the methods could indeed tolerate high correlations, given a sufficient SNR, but failed when synchronous sources were present. The success rates of the methods with data containing highly correlated sources were qualitatively as in Fig. 3, but decreased faster as function of SNR. A brief description of the effects of temporal correlations and linear dependence of source time-courses on the visibility of such signal sources in a topographical scanning that applies data covariance matrix, like beamformers and MUSIC, has been recently presented by Mäkelä et al. (2017). Special techniques can be used for analyzing highly correlated or synchronous sources (*e.g.*, see (Diwakar et al., 2011; Brookes et al., 2007)), but this was out of the scope of this study.

Conclusion

We introduced the TRAP-MUSIC method, which provides a solution to the RAP dilemma, a hidden limitation that we found in RAP-MUSIC. TRAP-MUSIC was successfully applied in source estimation with simulated EEG and MEG and measured MEG data. We argue that TRAP-MUSIC is an efficient and robust tool for locating multiple sources; the method is suitable even for real-time analysis.

Acknowledgments

This study was funded by Academy of Finland (grant number 283105), Foundation for Aalto University Science and Technology, and Oskar Öflund Foundation.

References

Ahlfors, S.P., Ilmoniemi, R.J., Hämäläinen, M.S., 1992. Estimates of visually evoked cortical currents. Electroencephalogr. Clin. Neurophysiol. 82 (3), 225–236.
Baker, A.P., Brookes, M.J., Rezek, I.A., Smith, S.M., Behrens, T., Smith, P.J.P., Woolrich, M., 2014. Fast transient networks in spontaneous human brain activity. Elife 3, e01867.
Birbaumer, N., Murguialday, A.R., Weber, C., Montoya, P., 2009. Neurofeedback and brain–computer interface: clinical applications. Int. Rev. Neurobiol. 86, 107–117.
Birot, G., Albera, L., Wendling, F., Merlet, I., 2011. Localization of extended brain sources from EEG/MEG: the ExSo-MUSIC approach. NeuroImage 56 (1), 102–113.
Brookes, M.J., Stevenson, C.M., Barnes, G.R., Hillebrand, A., Simpson, M.I., Francis, S.T., Morris, P.G., 2007. Beamformer reconstruction of correlated sources using a modified source model. NeuroImage 34 (4), 1454–1465.
Cheyne, D., Bakhtazad, L., Gaetz, W., 2006. Spatiotemporal mapping of cortical activity accompanying voluntary movements using an event-related beamforming approach. Hum. Brain Mapp. 27 (3), 213–229.
Dannhauer, M., Lanfer, B., Wolters, C.H., Knösche, T.R., 2011. Modeling of the human skull in EEG source analysis. Hum. Brain Mapp. 32 (9), 1383–1399.
Dinh, C., Strohmeier, D., Esch, L., Guellmar, D., Baumgarten, D., Hämäläinen, M., Haueisen, J., 2014. Real-time single-trial source localization using RAP-MUSIC and region of interest clustering. Biomed. Engineering/Biomedizinische Tech. 59. S949–S949.
Dinh, C., Strohmeier, D., Haueisen, J., Güllmar, D., 2012. Brain atlas based region of interest selection for real-time source localization using K-means lead field clustering and RAP-MUSIC. Biomed. Engineering/Biomedizinische Tech. 57 (SI-1 Track-O), 813–813.
Dinh, C., Strohmeier, D., Luessi, M., Güllmar, D., Baumgarten, D., Haueisen, J., Hämäläinen, M.S., 2015. Real-time MEG source localization using regional clustering. Brain Topogr. 28 (6), 771–784.
Diwakar, M., Tal, O., Liu, T.T., Harrington, D.L., Srinivasan, R., Muzzatti, L., Song, T., Theilmann, R.J., Lee, R.R., Huang, M.-X., 2011. Accurate reconstruction of temporal correlation for neuronal sources using the enhanced dual-core MEG beamformer. NeuroImage 56 (4), 1918–1928.
Ewald, A., Avarvand, F.S., Nolte, G., 2014. Wedge MUSIC: a novel approach to examine experimental differences of brain source connectivity patterns from EEG/MEG data. NeuroImage 101, 610–624.
Fang, Q., Boas, D.A., 2009. Tetrahedral mesh generation from volumetric binary and grayscale images. In: Biomedical Imaging: from Nano to Macro, 2009. ISBI'09. IEEE International Symposium on. IEEE, pp. 1142–1145.
Fischl, B., 2012. Freesurfer. NeuroImage 62 (2), 774–781.
Gonçalves, S.I., de Munck, J.C., Verbunt, J.P., Bijma, F., Heethaar, R.M., da Silva, F.L., 2003. In vivo measurement of the brain and skull resistivities using an eit-based method and realistic models for the head. IEEE Trans. Biomed. Eng. 50 (6), 754–767.
Gramfort, A., Luessi, M., Larson, E., Engemann, D.A., Strohmeier, D., Brodbeck, C., Parkkonen, L., Hämäläinen, M.S., 2014. MNE software for processing MEG and EEG data. NeuroImage 86, 446–460.

Groß, J., Kujala, J., Hämäläinen, M., Timmermann, L., Schnitzler, A., Salmelin, R., 2001. Dynamic imaging of coherent sources: studying neural interactions in the human brain. Proc. Natl. Acad. Sci. 98 (2), 694–699.
Hämäläinen, M., Hari, R., Ilmoniemi, R.J., Knuutila, J., Lounasmaa, O.V., 1993. Magnetoencephalography—theory, instrumentation, and applications to noninvasive studies of the working human brain. Rev. Mod. Phys. 65 (2), 413–496.
Hämäläinen, M.S., Sarvas, J., 1989. Realistic conductivity geometry model of the human head for interpretation of neuromagnetic data. Biomed. Eng. IEEE Trans. 36 (2), 165–171.
Kaipio, J., Somersalo, E., 2007. Statistical inverse problems: discretization, model reduction and inverse crimes. J. Comput. Appl. Math. 198 (2), 493–504.
Katyal, B., Schimpf, P.H., 2004. Multiple current dipole estimation in a realistic head model using R-MUSIC. In: Engineering in Medicine and Biology Society, 2004. IEMBS'04. 26th Annual International Conference of the IEEE, vol. 1. IEEE, pp. 829–832.
Liu, H., Schimpf, P.H., 2006. Efficient localization of synchronous EEG source activities using a modified RAP-MUSIC algorithm. Biomed. Eng. IEEE Trans. 53 (4), 652–661.
Mäkelä, N., Sarvas, J., Ilmoniemi, R.J., 2017. A simple reason why beamformer may (not) remove the tACS-induced artifact in MEG (in Proceedings, Neuromodulation NYC 2017 Conference). Brain Stimul. 10 (4), e66–e67.
Mauguiere, F., Merlet, I., Forss, N., Vanni, S., Jousmäki, V., Adeleine, P., Hari, R., 1997. Activation of a distributed somatosensory cortical network in the human brain. a dipole modelling study of magnetic fields evoked by median nerve stimulation. part I: location and activation timing of SEF sources. Electroencephalogr. Clin. Neurophysiol./Evoked Potentials Sect. 104 (4), 281–289.
Moiseev, A., Gaspar, J.M., Schneider, J.A., Herdman, A.T., 2011. Application of multi-source minimum variance beamformers for reconstruction of correlated neural activity. NeuroImage 58 (2), 481–496.
Mosher, J.C., Leahy, R.M., 1998. Recursive MUSIC: a framework for EEG and MEG source localization. Biomed. Eng. IEEE Trans. 45 (11), 1342–1354.
Mosher, J.C., Leahy, R.M., 1999. Source localization using recursively applied and projected (RAP) MUSIC. Signal Process. IEEE Trans. 47 (2), 332–340.
Mosher, J.C., Leahy, R.M., Lewis, P.S., 1999. EEG and MEG: forward solutions for inverse methods. Biomed. Eng. IEEE Trans. 46 (3), 245–259.
Nakamura, A., Yamada, T., Goto, A., Kato, T., Ito, K., Abe, Y., Kachi, T., Kakigi, R., 1998. Somatosensory homunculus as drawn by MEG. NeuroImage 7 (4), 377–386.
Pascarella, A., Sorrentino, A., Campi, C., Piana, M., 2010. Particle filtering, beamforming and RAP-MUSIC in the analysis of magnetoencephalography time series: a comparison of algorithms. Inverse Probl. Imag. 4, 169–190.
Sanchez, G., Daunizeau, J., Maby, E., Bertrand, O., Bompas, A., Mattout, J., 2014. Toward a new application of real-time electrophysiology: online optimization of cognitive neurosciences hypothesis testing. Brain Sci. 4 (1), 49–72.
Schmidt, R.O., 1986. Multiple emitter location and signal parameter estimation. Antenn. Propag. IEEE Trans. 34 (3), 276–280.
Sekihara, K., Nagarajan, S.S., 2008. Adaptive Spatial Filters for Electromagnetic Brain Imaging. Springer Science & Business Media.
Shahbazi, F., Ewald, A., Nolte, G., 2015. Self-consistent MUSIC: an approach to the localization of true brain interactions from EEG/MEG data. NeuroImage 112, 299–309.
Sharon, D., Hämäläinen, M.S., Tootell, R.B., Halgren, E., Belliveau, J.W., 2007. The advantage of combining MEG and EEG: comparison to fMRI in focally stimulated visual cortex. NeuroImage 36 (4), 1225–1235.
Stenroos, M., Sarvas, J., 2012. Bioelectromagnetic forward problem: isolated source approach revis(it)ed. Phys. Med. Biol. 57 (11), 3517–3535.
Taulu, S., Kajola, M., Simola, J., 2004. Suppression of interference and artifacts by the signal space separation method. Brain Topogr. 16 (4), 269–275.
Vrba, J., Robinson, S.E., 2000. Linearly constrained minimum variance beamformers, synthetic aperture magnetometry, and MUSIC in MEG applications. In: Conference Record of the Thirty-fourth Asilomar Conference on Signals, Systems and Computers, vol. 1. IEEE, pp. 313–317.